

Testing GR with the Double Pulsar: Recent Results

M. Kramer, D.R. Lorimer, A.G. Lyne, M. McLaughlin
University of Manchester, Jodrell Bank Observatory, UK

M. Burgay, N. D'Amico, A. Possenti
INAF - Osservatorio Astronomica di Cagliari, Italy

F. Camilo
Columbia Astrophysics Laboratory, Columbia University, USA

P.C.C. Freire
NAIC, Arecibo Observatory, USA

B.C. Joshi
NCRA, Pune, India

R.N. Manchester, J. Reynolds, J. Sarkissian
Australia Telescope National Facility, CSIRO, Australia

I.H. Stairs, R. D. Ferdman
Department of Physics and Astronomy, University of British Columbia, Canada

This first ever double pulsar system consists of two pulsars orbiting the common center of mass in a slightly eccentric orbit of only 2.4-hr duration. The pair of pulsars with pulse periods of 22 ms and 2.8 sec, respectively, confirms the long-proposed recycling theory for millisecond pulsars and provides an exciting opportunity to study the works of pulsar magnetospheres by a very fortunate geometrical alignment of the orbit relative to our line-of-sight. In particular, this binary system represents a truly unique laboratory for relativistic gravitational physics. This contribution serves as an update on the currently obtained results and their consequences for the test of general relativity in the strong-field regime. A complete and more up-to-date report of the timing results will be presented elsewhere shortly.

1. INTRODUCTION

In this year 2005 we celebrate the work of Albert Einstein, remembering his enormous contribution to our understanding of nature and the Universe. One of the best ways for honoring his work is to point out that still today, a hundred of years later, hundreds of scientists around the world are deeply involved in searching for the limits up to which his centennial theory of general relativity (GR) can be applied. To date GR has passed all observational tests with flying colours. Still, it is the continued aim of many physicists to achieve more stringent tests by either increasing the precision of the tests or by testing different aspects. Some of the most stringent tests are obtained by satellite experiments in the solar system. One must not forget, however, that these solar-system experiments are all made in the gravitational weak-field regime and that they will never be able to provide tests in the strong-field limit where deviations from GR may appear more clearly or even for the first time (see e.g. [1]). This strong-field regime is best explored using radio pulsars.

Pulsars, highly magnetized rotating neutron stars, are unique and versatile objects which can be used to study an extremely wide range of physical and astrophysical problems. Beside testing theories of gravity one can study the Galaxy and the interstellar medium, stars, binary systems and their evolution, plasma physics and solid state physics under extreme conditions. In these proceedings, we will present such applications for gravitational physics made possible

by the first ever discovered double pulsar [2, 3]. We will demonstrate that this rare binary system represents a truly unique laboratory for relativistic gravity. We will present an update on the currently obtained timing results and their consequences for tests of GR. A complete and more up-to-date report of the timing results will be presented elsewhere shortly.

2. THE DOUBLE PULSAR

Our team discovered the 22.8-ms pulsar J0737–3039 in April 2003 [2] in an extension to the hugely successful Parkes Multi-beam survey [4]. It was soon found to be a member of the most extreme relativistic binary system ever discovered: its short orbital period ($P_b = 2.4$ hrs) is combined with a remarkably high value of periastron advance ($\dot{\omega} = 16.9 \text{ deg yr}^{-1}$, i.e. four times larger than for PSR B1913+16!) that was measurable after only a few days of observations. The system parameters predict that the two members of the binary system will coalesce on a short time scale of only ~ 85 Myr. This boosts the hopes for detecting a merger of two neutron stars with first-generation ground-based gravitational wave detectors by a factor of several compared to previous estimates based on only the double neutron stars B1534+12 and B1913+16 [2, 5].

In October 2003, we detected radio pulses from the second neutron star when data sets covering the full orbital period were analysed [3]. The reason why signals from the 2.8-s pulsar companion (now called PSR

J0737–3039B, hereafter “B”) to the millisecond pulsar (now called PSR J0737–3039A, hereafter “A”) had not been found earlier, became clear when it was realized that B was only bright for two short parts of the orbit. For the remainder of the orbit, the pulsar B is extremely weak and only detectable with the most sensitive equipment. The detection of a young companion B around an old millisecond pulsar A confirms the evolution scenario proposed for recycled pulsars (e.g. [6, 7]) and made this already exciting system sensational, providing a truly unique testbed for relativistic gravity.

3. STRONG-FIELD TESTS OF GENERAL RELATIVITY

Since neutron stars are very compact massive objects, the double pulsar (and other double neutron star systems) can be considered as almost ideal point sources for testing theories of gravity in the strong-gravitational-field limit. Tests can be performed when

a number of relativistic corrections to the Keplerian description of an orbit, the so-called “post-Keplerian” (PK) parameters, can be measured. For point masses with negligible spin contributions, the PK parameters in each theory should only be functions of the a priori unknown neutron star masses and the well measurable Keplerian parameters.

With the two masses as the only free parameters, the measurement of three or more PK parameters over-constrains the system, and thereby provides a test ground for theories of gravity. In a theory that describes a binary system correctly, the PK parameters produce theory-dependent lines in a mass-mass diagram that all intersect in a single point.

As A has the faster pulse period (and is bright throughout the entire orbit apart from a ~ 27 -s eclipse at superior conjunction), we can time A much more accurately than B and measure precise PK parameters for A’s orbit. In GR, the five most important PK parameters are given to first post-Newtonian (1PN, or $\mathcal{O}(v^2/c^2)$) order by [8]:

$$\dot{\omega} = 3T_{\odot}^{2/3} \left(\frac{P_b}{2\pi} \right)^{-5/3} \frac{1}{1-e^2} (M_A + M_B)^{2/3}, \quad (1)$$

$$\gamma = T_{\odot}^{2/3} \left(\frac{P_b}{2\pi} \right)^{1/3} e \frac{M_B(M_A + 2M_B)}{(M_A + M_B)^{4/3}}, \quad (2)$$

$$\dot{P}_b = -\frac{192\pi}{5} T_{\odot}^{5/3} \left(\frac{P_b}{2\pi} \right)^{-5/3} \frac{(1 + \frac{73}{24}e^2 + \frac{37}{96}e^4)}{(1-e^2)^{7/2}} \frac{M_A M_B}{(M_A + M_B)^{1/3}}, \quad (3)$$

$$r = T_{\odot} M_B, \quad (4)$$

$$s = T_{\odot}^{-1/3} \left(\frac{P_b}{2\pi} \right)^{-2/3} x \frac{(M_A + M_B)^{2/3}}{M_B}, \quad (5)$$

where P_b is the period and e the eccentricity and x the semi-major axis measured in light-s of the binary orbit. The masses M_A and M_B of A and B, respectively, are expressed in solar masses (M_{\odot}). We define the constant $T_{\odot} = GM_{\odot}/c^3 = 4.925490947\mu\text{s}$ where G denotes the Newtonian constant of gravity and c the speed of light. The first PK parameter, $\dot{\omega}$, is the easiest to measure and describes the relativistic advance of periastron. According to Eqn. 1 it provides an immediate measurement of the total mass of the system, $(M_A + M_B)$. The parameter γ denotes the amplitude of delays in arrival times caused by the varying effects of the gravitational redshift and time dilation (second order Doppler) as the pulsar moves in its elliptical orbit at varying distances from the companion and with varying speeds. The decay of the orbit due to gravitational wave damping is expressed by the change in

orbital period, \dot{P}_b . The other two parameters, r and s , are related to the Shapiro delay caused by the gravitational field of the companion. These parameters are only measurable, depending on timing precision, if the orbit is seen nearly edge-on. For pulsar A, all these quantities have indeed been measured, providing a large number of available tests. In fact, in addition to tests with these PK parameters, the possibility to measure the orbit of both A and B opens up opportunities that go well beyond what is possible with previously known double neutron stars, as we will describe now.

With a measurement of the projected semi-major axes of the orbits of both A and B, we obtain a precise measurement of the mass ratio, $R(M_A, M_B)$, from Kepler’s third law,

$$R(M_A, M_B) \equiv M_A/M_B = x_B/x_A. \quad (6)$$

For every realistic theory of gravity, we can expect the mass ratio, R , to follow this simple relation [9], at least to 1PN order. Most importantly, the R value is not only theory-independent, but also independent of strong-field (self-field) effects which is not the case for PK-parameters. This provides a stringent and new constraint for tests of gravitational theories as any combination of masses derived from the PK-parameters *must* be consistent with the mass ratio derived from Kepler’s 3rd law. With five PK parameters already available, this additional constraint makes the double pulsar the most overdetermined system to date where the most relativistic effects can be studied in the strong-field limit.

4. TIMING OF THE DOUBLE PULSAR

Our observations already provide measurements for all five PK parameters listed above. This includes a measurement of an orbital decay of the binary orbit due to gravitational wave emission with a rate of 7mm/day. As indicated earlier, we can use these results to test GR in a very elegant way [9]. The unique relationship between the two masses of the system predicted by GR (or any other theory) for each PK parameter can be plotted in a diagram showing the mass of A on one axis and B on the other. We expect all curves, including that of the mass ratio R , to intersect in a single point if the chosen theory (here GR) is a valid description of the nature of this system. Such tests have been possible to date in PSR B1913+16 (e.g. [10]) and for PSR B1534+12 (e.g. [11]). However, in neither of these systems were so many curves available as for the double pulsar system for which we derive a $M_A - M_B$ plot as shown in Fig. 1.

It turns out that, as another stroke of luck, we are observing the system almost completely edge-on which allows us to determine a Shapiro delay to very high precision. It also means, however, that we can probe a pulsar magnetosphere for the very first time using a background beacon. Results of the magnetospheric interactions between A and B [12] and the eclipse of A’s signal at its superior conjunction [3, 13, 14] have been presented elsewhere and must be considered in search for a possible contamination of the timing data and hence a violation of our assumption that we deal with a “clean” system of point sources.

While all studies so far confirm the cleanness of the system, we also have to consider that the times-of-arrival (TOAs) are obtained with a standard “template matching” procedure that involves a cross-correlation of the observed pulse profile with high signal-to-noise ratio template (e.g. [15]). Any change in the pulse profile could therefore lead to systematic variations in the measured TOAs. For this reason it

was necessary to perform detailed studies of the profiles of A and B and to investigate any possible profile evolution with time. Indeed, profile changes on secular time scales are expected for the double pulsar for the following reason.

In GR, the proper reference frame of a freely falling object suffers a precession with respect to a distant observer, called geodetic precession. In a binary pulsar system this geodetic precession leads to a relativistic spin-orbit coupling, analogous of spin-orbit coupling in atomic physics [16]. As a consequence, the pulsar spins precess about the total angular momentum, changing the relative orientation of the pulsars to one another and toward Earth. Since the orbital angular momentum is much larger than the pulsars’ angular momenta, the total angular momentum is practically represented by the orbital angular momentum. The precession rate [17] depends on the period and the eccentricity of the orbit as well as the masses of A and B. With the orbital parameters of the double pulsar, GR predicts precession periods of only 75 yr for A and 71 yr for B.

Geodetic precession should have a direct effect on the timing as it causes the polar angles of the spins and hence the effects of aberration to change with time [9]. These changes modify the *observed* orbital parameters, like projected semi-major axis and eccentricity, which differ from the *intrinsic* values by an aberration dependent term, potentially allowing us to infer the system geometry [18]. Other consequences of geodetic precession can be expected to be detected much sooner and are directly relevant for the timing of A and B. These arise from variations in the pulse shape due to changing cuts through the emission beam as the pulsar spin axes precess. Moreover, geodetic precession also leads to a change in the relative alignment of the pulsar magnetospheres, so that the visibility pattern or even the profile of B may vary due to these changes as well.

The possibility to observe such phenomena is exciting but requires a careful analysis to exclude any impact onto the timing of the two pulsars. Indeed, the necessity to check for these effects has delayed the publication of the currently final timing results of the double pulsar. The analysis is now almost complete and results will be published shortly. A preliminary update is given in Table 1 and discussed below.

5. PRESENT RESULTS

The study of the profile evolution of A [19] did not lead to the detection of any profile change over a period of 15 months. This present non-detection greatly simplifies the timing of A but does not exclude the possibility that changes may not happen in the future. While the effects of geodetic precession could be small due to a near alignment of pulsar A’s spin

Table I Observed and derived parameters of PSRs J0737–3039A and B. Standard errors are given in parentheses after the values and are in units of the least significant digit(s).

Pulsar	PSR J0737–3039A	PSR J0737–3039B
Pulse period P (ms)	22.699378556138(2)	2773.4607474(4)
Period derivative \dot{P}	$1.7596(2) \times 10^{-18}$	$0.88(13) \times 10^{-15}$
Epoch of period (MJD)	52870.0	
Right ascension α (J2000)	$07^{\text{h}}37^{\text{m}}51^{\text{s}}.24795(2)$	
Declination δ (J2000)	$-30^{\circ}39'40''.7247(6)$	
Orbital period P_b (day)	0.1022515628(2)	
Eccentricity e	0.087778(2)	
Epoch of periastron T_0 (MJD)	52870.0120588(3)	
Advance of periastron $\dot{\omega}$ (deg yr $^{-1}$)	16.900(2)	
Longitude of periastron ω (deg)	73.805(1)	$73.805 + 180.0$
Projected semi-major axis $x = asini/c$ (sec)	1.415032(2)	1.513(4)
Gravitational redshift parameter γ (ms)	0.39(2)	
Shapiro delay parameter $s = \sin i$	0.9995(4)	
Shapiro delay parameter r (μs)	6.2(6)	
Orbital decay \dot{P}_b (10^{-12})	$-1.20(8)$	
Mass ratio $R = M_A/M_B$	1.071(1)	

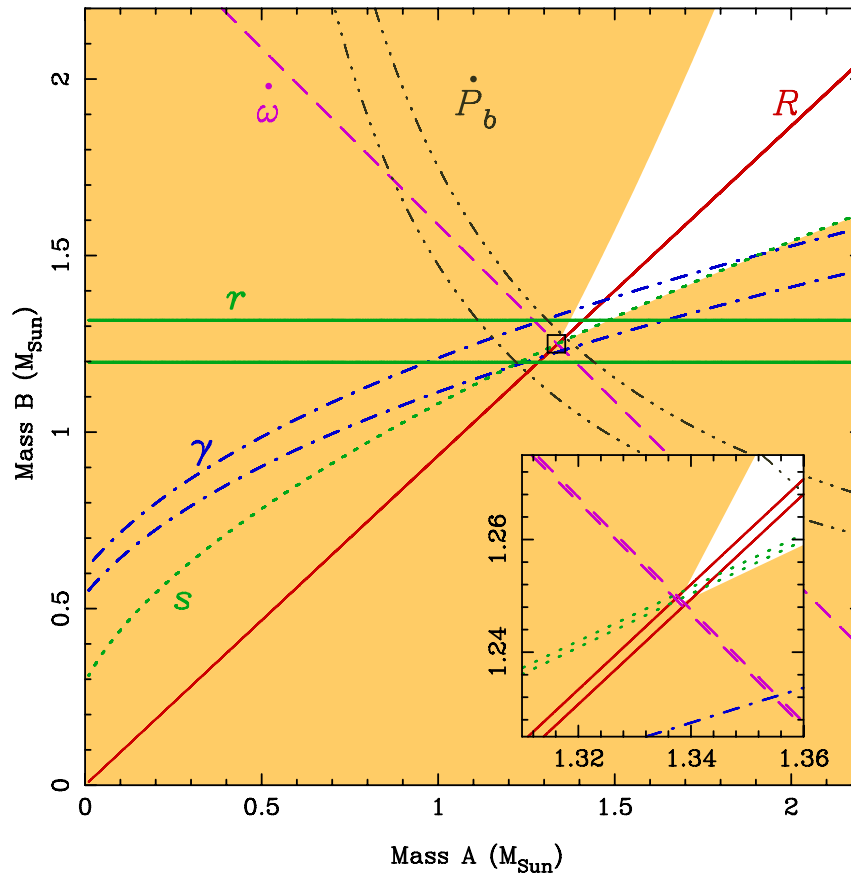


Figure 1: ‘Mass-mass’ diagram showing the observational constraints on the masses of the neutron stars in the double pulsar system J0737–3039. The shaded regions are those that are excluded by the Keplerian mass functions of the two pulsars. Further constraints are shown as pairs of lines enclosing permitted regions as given by the observed mass ratio and PK parameters shown here as predicted by general relativity. Inset is an enlarged view of the small square encompassing the intersection of these constraints (see text).

and the orbital momentum vector, the results could also be explained by observing the system at a particular precession phase. While this case appears to be relatively unlikely, it must not be excluded as such a situation had indeed occurred for PSR B1913+16 [20]. Indeed, a modelling of the results suggests that this present non-detection of profile changes is consistent with a rather wide range of possible system geometries. One conclusion that can be drawn, however, is that the observations are inconsistent with the large profile changes that had been predicted by some models [21].

In contrast to the results for A, similar studies of the profile evolution of B [22] reveal a clear evolution of B's emission on orbital and secular time-scales. The profile of B is changing with time, while also the light-curves of B (i.e. the visibility of B versus orbital phase) undergo clear changes. These phenomena may be caused by a changing magnetospheric interaction due to geometry variations resulting from geodetic precession. In any case, these changes require sophisticated timing analysis techniques and the preliminary results obtained with this techniques are listed in Table 1, while final results will be published shortly.

The present timing results already indicate that the proper motion of this system is surprisingly small. While a significant measurement of a proper motion vector via pulsar timing will be available shortly, the present limit suggests a systemic velocity of less than 30 km/s for a dispersion measure distance of 600 pc [23].¹ While such a small velocity may be indicative of a small kick imparted onto B during its supernova explosion [25], other studies find this limit still to be consistent with a kick of average magnitude [26]. In any case, such a small velocity is good news for tests of GR. Usually, the observed value of \dot{P}_b is positively biased by an effect known as secular acceleration arising from a relative motion and acceleration of the system (e.g. [27]). Computing the magnitude of this observational bias using the obtained limit on the proper motion, however, suggests that the contribution is much less than 1%, so that the orbital decay measurement will be available for another precise GR test.

Finally, scintillation measurements have recently suggested an orbital inclination angle that is extremely close to 90 deg (i.e. within (0.29 ± 0.14) deg) [24]. This measurement appears to be inconsistent with results from the timing observations and the measurement of the Shapiro delay parameter, $s = \sin i$, which suggest an inclination angle that is close but significantly different from 90 deg. One should note that the scintillation results are based on corre-

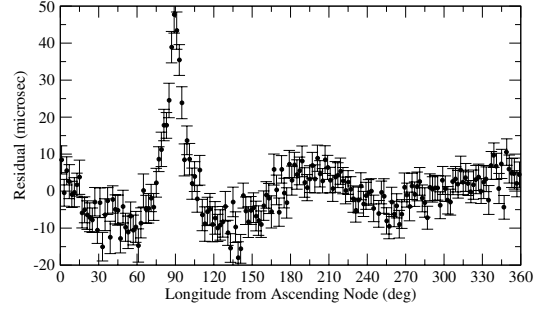


Figure 2: The effect of the Shapiro delay caused by the gravitational potential of B seen in the timing residuals of A. The timing residuals obtained by fitting all model parameters shown in Table 1 except the Shapiro delay parameters r and s . The left-over structure represents the higher harmonics of the Shapiro delay that are unabsorbed by fits to the Keplerian parameters.

lating the scintillation properties of A and B over the short time-span of the orbital motion when they are in conjunction to the observer. In contrast, the measurement of the inclination angle from timing measurements results from detecting significant harmonic structure in the post-fit residuals after parts of the Shapiro delay effect are absorbed in the fit for the Römer delay, i.e. the light travel time across the orbit. As shown in Figure 2, these structures are present throughout the whole orbit, so that the results from timing measurements may be expected to be more reliable. We are currently studying the origin of this apparent inconsistency between these two methods, checking both any contamination of the Shapiro delay measurements and effects influencing the scintillation results. An exciting possibility could be that the emission of A suffers measurable refraction while propagating through the magnetosphere of B. If that were indeed the case, we would have a direct handle onto the magneto-ionic properties of B's magnetosphere for the first time.

Inspecting the results shown in Table 1, we can take the most precise parameters (i.e. the mass ratio R , the advance of periastron $\dot{\omega}$ and the Shapiro delay parameter s) to test theories of gravity. Assuming that GR is the correct theory of gravitation, we use Eqn. 1 to derive the total mass of the system and combine it with the observed mass ratio to obtain $M_A = 1.338 \pm 0.001 M_\odot$ and $M_B = 1.249 \pm 0.001 M_\odot$. Using these precisely determined masses we compute the Shapiro delay parameter s as predicted by GR and compare it to the observed value. We find that $s^{\text{GR}}/s^{\text{obs}} = 1.0002^{+0.0011}_{-0.0006}$. Hence, GR passes this test at the 0.1% level. This is the most stringent test of GR in the strong-field limit so far.

¹We note that this small velocity is consistent with the 66 km/s derived from scintillation measurements as the latter value is not corrected for a relative motion of the Earth [24].

6. FUTURE

In the near and far future, the precision of the determined parameters will increase further, simply by the available longer time span but also by the potential employment of better instrumentation. In a few years, we should be able to measure additional PK parameters, including those which arise from a relativistic deformation of the pulsar orbit (resulting in angular and radial orbital eccentricities) and those which find their origin in aberration effects and their interplay with geodetic precession (see [9]). On secular time scales we will even achieve a precision that will require us to consider post-Newtonian terms that go beyond the currently used description of the PK parameters. Indeed, the equations for the PK parameters given earlier are only correct to lowest PN order. However, higher-order corrections are expected to become important if timing precision is sufficiently high. While this has not been the case in the past, the double pulsar system may allow measurements of these effects in the future [3].

One such effect involves the prediction by GR that, in contrast to Newtonian physics, the neutron stars' spins affect their orbital motion via spin-orbit coupling. This effect would be visible most clearly as a contribution to the observed $\dot{\omega}$ in a secular [17] and periodic fashion [28]. For the J0737–3039 system, the expected contribution is about an order of magnitude larger than for PSR B1913+16, i.e. $2 \times 10^{-4} \text{ deg yr}^{-1}$ (for A, assuming a geometry as determined for PSR B1913+16 [20]). As the exact value depends on the pulsars' moment of inertia, a potential measurement of this effect allows the moment of inertia of a neutron star to be determined for the first time [29].

If two parameters, e.g. the Shapiro parameter s and the mass ratio R , can be measured sufficiently accurately, an expected $\dot{\omega}_{\text{exp}}$ can be computed from the intersection point. This value can be compared to the observed value $\dot{\omega}_{\text{obs}}$ which is given by (see [29])

$$\dot{\omega}_{\text{obs}} = \dot{\omega}_{1\text{PN}} [1 + \Delta\dot{\omega}_{2\text{PN}} - g^A \Delta\dot{\omega}_{\text{SO}}^A - g^B \Delta\dot{\omega}_{\text{SO}}^B] \quad (7)$$

where the last two terms represent contributions from the pulsar spin. In these terms, $g^{A,B}$ are geometry dependent factors whilst $\Delta\dot{\omega}_{\text{SO}}^{A,B}$ arise from relativistic spin-orbit coupling, formally at the 1PN level. However, it turns out that for binary pulsars these effects have a magnitude equivalent to 2PN effects [28], so that they only need to be considered if $\dot{\omega}$ is to be studied at this higher level of approximation. We find $\Delta\dot{\omega}_{\text{SO}} \propto I/PM^2$ [29], so that with precise masses M the moment of inertia I can be measured and the neutron star “equation-of-state” and our understanding of matter at extreme pressure and densities can be tested.

The dependence of $\Delta\dot{\omega}_{\text{SO}}$ on the spin period P suggests that only a measurement for pulsar A can be

obtained. It also requires that at least two other parameters can be measured to a similar accuracy as $\dot{\omega}$. Despite being a tough challenge, e.g. due to the expected profile variation caused by geodetic precession, the prospects are promising. Simulations indicate that a few years of high precision timing are sufficient.

7. SUMMARY & CONCLUSIONS

With the measurement of five PK parameters and the unique information about the mass ratio, the PSR J0737–3039 system provides a truly unique test-bed for relativistic theories of gravity. So far, GR also passes this test with flying colors. The precision of this test and the nature of the resulting constraints go beyond what has been possible with other systems in the past. The test achieved so far is, however, only the beginning of a study of relativistic phenomena that can be investigated in great detail in this wonderful cosmic laboratory.

Acknowledgments

MK is grateful for the local support provided by the conference organisers.

References

- [1] T. Damour, G. Esposito-Farèse, Phys. Rev. D 58 (042001) 1–12 (1998).
- [2] M. Burgay, N. D’Amico, A. Possenti, R. N. Manchester, A. G. Lyne, B. C. Joshi, M. McLaughlin, M. Kramer, J. M. Sarkissian, F. Camilo, V. Kalogera, C. Kim, D. R. Lorimer, Nature 426 531–533 (2003).
- [3] A. G. Lyne, M. Burgay, M. Kramer, A. Possenti, R. N. Manchester, F. Camilo, M. McLaughlin, D. R. Lorimer, B. C. Joshi, J. E. Reynolds, P. C. C. Freire, Science 303 1153–1157 (2004).
- [4] R. N. Manchester, A. G. Lyne, F. Camilo, J. F. Bell, V. M. Kaspi, N. D’Amico, N. P. F. McKay, F. Crawford, I. H. Stairs, A. Possenti, D. J. Morris, D. C. Sheppard, MNRAS 328 17–35 (2001).
- [5] V. Kalogera, C. Kim, D. R. Lorimer, M. Burgay, N. D’Amico, A. Possenti, R. N. Manchester, A. G. Lyne, B. C. Joshi, M. A. McLaughlin, M. Kramer, J. M. Sarkissian, F. Camilo, ApJ 601 L179–L182 (2004).
- [6] G. S. Bisnovatyi-Kogan, B. V. Komberg, Sov. Astron. 18 217–221 (1974).
- [7] L. L. Smarr, R. Blandford, ApJ 207 574–588 (1976).
- [8] T. Damour, N. Deruelle, Ann. Inst. H. Poincaré (Physique Théorique) 44 263–292 (1986).

- [9] T. Damour, J. H. Taylor, *Phys. Rev. D* 45 1840–1868 (1992).
- [10] J. M. Weisberg, J. H. Taylor, The Relativistic Binary Pulsar B1913+16, in: M. Bailes, D. J. Nice, S. Thorsett (Eds.), *Radio Pulsars*, Astronomical Society of the Pacific, San Francisco, 2003, pp. 93–98.
- [11] I. H. Stairs, S. E. Thorsett, J. H. Taylor, A. Wolszczan, *ApJ* 581 501–508 (2002).
- [12] M. A. McLaughlin, M. Kramer, A. G. Lyne, D. R. Lorimer, I. H. Stairs, A. Possenti, R. N. Manchester, P. C. C. Freire, B. C. Joshi, M. Burgay, F. Camilo, N. D’Amico, *ApJ* 613 L57–L60 (2004).
- [13] V. M. Kaspi, S. M. Ransom, D. C. Backer, R. Ramachandran, P. Demorest, J. Arons, A. Spitkovsky, *ApJ* 613 L137–L140 (2004).
- [14] M. A. McLaughlin, A. G. Lyne, D. R. Lorimer, A. Possenti, R. N. Manchester, F. Camilo, I. H. Stairs, M. Kramer, M. Burgay, N. D’Amico, P. C. C. Freire, B. C. Joshi, N. D. R. Bhat, *ApJ* 616 L131–L134 (2004).
- [15] J. H. Taylor, *Philos. Trans. Roy. Soc. London A* 341 117–134 (1992).
- [16] T. Damour, R. Ruffini, *C. R. Acad. Sc. Paris, Serie A* 279 971–973 (1974).
- [17] B. M. Barker, R. F. O’Connell, *ApJ* 199 L25 (1975).
- [18] I. H. Stairs, S. E. Thorsett, Z. Arzoumanian, *Physical Review Letters*, 93 (14) 141101 (2004).
- [19] R. N. Manchester, M. Kramer, A. Possenti, A. G. Lyne, M. Burgay, I. H. Stairs, A. W. Hotan, M. A. McLaughlin, D. R. Lorimer, G. B. Hobbs, J. M. Sarkissian, N. D’Amico, F. Camilo, B. C. Joshi, P. C. C. Freire, *ApJ* 621 L49–L52 (2005).
- [20] M. Kramer, *ApJ* 509 856–860 (1998).
- [21] F. A. Jenet, S. M. Ransom, *Nature* 428 919–921 (2004).
- [22] M. Burgay, A. Possenti, R. N. Manchester, M. Kramer, M. A. McLaughlin, D. R. Lorimer, I. H. Stairs, B. C. Joshi, A. G. Lyne, F. Camilo, N. D’Amico, P. C. C. Freire, J. M. Sarkissian, A. W. Hotan, G. B. Hobbs, submitted to *ApJL*.
- [23] J. M. Cordes, T. J. W. Lazio, submitted *astro-ph/0207156*
- [24] W. A. Coles, M. A. McLaughlin, B. J. Rickett, A. G. Lyne, N. D. R. Bhat, *ApJL*, in press.
- [25] T. Piran, N. J. Shaviv, *Physical Review Letters* 94 (5) 051102–+ (2005).
- [26] B. Willems, V. Kalogera, submitted to *Physical Review Letters*.
- [27] T. Damour, J. H. Taylor, *ApJ* 366 501–511 (1991).
- [28] N. Wex, *Class. Quantum Grav.* 12 983 (1995).
- [29] T. Damour, G. Schäfer, *Nuovo Cim.* 101 127 (1988).